Table I. Rates of *p*-Nitrophenyl Acetate Hydrolysis Catalyzed by 1-Methylimidazole Before and After NO Addition

PHDME$^+$Cl$^-$ (μmol)	1-MeImid (μmol)	rate of ester hydrolysis before NO adn (ng/s)[a]	rate of ester hydrolysis after NO adn (ng/s)[a]
10	10	8.0	21.7
5	5	2.9	11.3
0	5		12.1[b]
5[c]	0	2.0[d]	2.2[d]
5[e]	5[e]	8.2	13.8

[a] Concentrations were calculated based upon aqueous solution of sodium *p*-nitrophenolate at pH 7.5. [b] No nitric oxide was added. [c] PHDME$^+$Cl$^-$ is not reduced. [d] This value corresponds to the rate of hydrolysis of *p*-nitrophenyl acetate by OH$^-$. [e] MCPH$^+$Cl$^-$ was used instead of PHDME$^+$Cl$^-$; the 5 μmol of imidazole is attached to the heme.

shown that addition of NO converts the carbonmonoxy-chelated heme to the five-coordinate iron(II)-NO complex (eq 3).[23] The

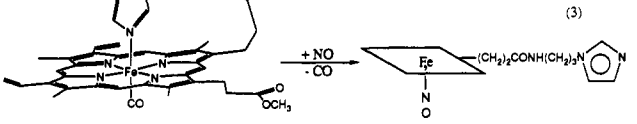

(3)

same change is observed for the 1-methylimidazole–protoheme–CO complex at low (<1 M) concentrations of 1-methylimidazole.[14] These observations suggest that the complexes might mimic the catalytic behavior of guanlyate cyclase.

We have chosen the general base-catalyzed hydrolysis of *p*-nitrophenyl acetate (pNPA)[24] to investigate the use of the model system as a trigger for such hydrolytic reactions. In order to facilitate the spectroscopic observation of *p*-nitrophenolate in the presence of optically dense heme solutions, we have carried out the reaction in a two-phase system. An aqueous buffer (3 mL at pH 7.5) was layered over a methylene chloride solution (0.3 mL) of either 5 μmol of chelated protoheme–CO (MCPH–CO) or 5 μmol of 1-methylimidazole–protoheme dimethyl ester–CO (Im-PHDME-CO). All experiments were under 1 atm of CO throughout. Reduction was accomplished with ascorbic acid. Gentle stirring of the methylene chloride layer (with a magnetic bar) was briefly interrupted at intervals to determine the absorbance of the upper layer. Figure 1 shows three absorbance versus time plots for a solution of chelated protoheme–CO: (1) in the absence of pNPA; (2) after its addition; and (3) after addition of NO gas (2 mL, 1 atm) to the aqueous phase. A similar series of plots for the 1:1 mixture of protoheme dimethyl ester and 1-methylimidazole under 1 atm of CO is also shown in Figure 1. The rates of *p*-nitrophenyl acetate hydrolysis for the control systems, in which either the heme or the 1-methylimidazole was absent, are given in Table I.

Figure 1 indicates an increase in the rate of hydrolysis upon the addition of NO which, as seen in Table I, is about the same as the rate increase upon addition of the same concentration of 1-methylimidazole. The heme alone does not alter the rate. Furthermore, the initial spectrum of the diluted heme from the reaction mixture is of imidazole–heme–CO, while the spectrum after hydrolysis corresponds to the heme–NO complex. It can be seen from Table I that the hydrolysis rate increase is proportional to the initial concentration of 1-MeIm-Hm-CO, as is expected if, upon addition of NO, all imidazole is released. Clearly, catalysis of this hydrolysis is due to released imidazole (as represented by eqs 4 and 5 for the 1-MeIm-Hm-CO).

Stimulation of imidazole catalysis of a hydrolytic reaction upon addition of NO to the chelated protoheme–CO complex represents an intriguing mechanism for biological catalysis. Although nitric oxide stimulation of guanylate cyclase might proceed by other mechanisms, our model presents a viable explanation. Continuing

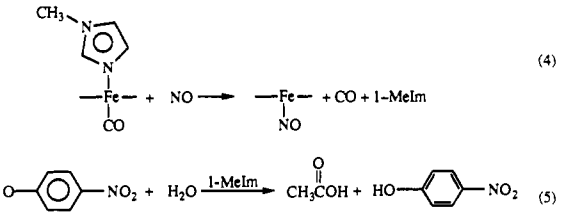

(4)

(5)

discoveries of the physiological effects of NO[25,26] suggest that both base catalysis and conformational triggering mechanisms might occur in biological systems.

Acknowledgment. We acknowledge the National Institutes of Health (Grants HL 13581 (T.G.T.) and HL 31159 (V.S.S.)) for support.

(23) Wu, G.-Z. Unpublished results.
(24) Blyth, C. A.; Knowles, J. R. *J. Am. Chem. Soc.* **1971**, *93*, 3021-3027.
(25) Brüne, B.; Lapetina, E. G. *J. Biol. Chem.* **1989**, *264*, 8455-8458.
(26) Lancaster, J. R., Jr.; Langrehr, J. M.; Bergonia, H. A.; Murase, N.; Simmons, R. L.; Hoffman, R. A. *J. Biol. Chem.* **1992**, *267*, 10994-10998.

A High-Potential Ferrous Complex and Its Conversion to an Alkylperoxoiron(III) Intermediate. A Lipoxygenase Model

Yan Zang, Timothy E. Elgren, Yanhong Dong, and Lawrence Que, Jr.*

Department of Chemistry, University of Minnesota Minneapolis, Minnesota 55455
Received October 16, 1992

Lipoxygenases are mononuclear non-heme iron enzymes which catalyze the peroxidation of fatty acids containing a 1,4-diene unit.[1] Spectroscopic evidence suggests that the native soybean lipoxygenase-1 possesses a six-coordinate high-spin Fe(II)[2,3] center with histidine and carboxylate ligands and a redox potential around 0.6 V vs NHE.[4] Treatment of the Fe(II) enzyme with product peroxide converts it to the active Fe(III) enzyme, which in turn reacts with excess peroxide to form a metastable purple species with λ_{max} = 570 nm.[1,5] In our efforts to model active sites of non-heme iron proteins, we have synthesized a high-spin ferrous complex that approximates the iron coordination environment proposed for native soybean lipoxygenase and affords a transient intermediate species upon treatment with alkyl hydroperoxide.

Reaction of equimolar amounts of $Fe(ClO_4)_2 \cdot 6H_2O$, TLA,[6,7] HOBz, and Et_3N in methanol/H_2O affords [Fe(TLA)(OBz)]ClO_4 (**1**)[8] as a light yellow powder. The structure of the BPh_4 salt[9]

(1) (a) Veldink, G. A.; Vliegenthart, J. F. G. *Adv. Inorg. Biochem.* **1984**, *6*, 139-161. (b) Feiters, M. C.; Boelens, H.; Veldink, G. A.; Vliegenthart, J. F. G.; Navaratnam, S.; Allen, J. C.; Nolting, H. F.; Hermes, C. *Recl. Trav. Chim. Pays-Bas* **1990**, *109*, 133-146.
(2) (a) Van der Heijdt, L. M.; Feiters, M. C.; Navaratnam, S.; Nolting, H. F.; Hermes, C.; Veldink, G. A.; Vliegenthart, J. F. G. *Eur. J. Biochem.* **1992**, *207*, 793-802. (b) Navaratnam, S.; Feiters, M. C.; Al-Hakim, M.; Allen, J. C.; Veldink, G. A.; Vliegenthart, J. F. G. *Biochim. Biophys. Acta* **1988**, *956*, 70-76.
(3) (a) Whittaker, J. W.; Solomon, E. I. *J. Am. Chem. Soc.* **1988**, *110*, 5329-5339. (b) Zhang, Y.; Gebhard, M. S.; Solomon, E. I. *J. Am. Chem. Soc.* **1991**, *113*, 5162-5175.
(4) Nelson, M. J. *Biochemistry* **1988**, *27*, 4273-4278.
(5) de Groot, J. J. M. C.; Garssen, G. J.; Veldink, G. A.; Vliegenthart, J. F. G.; Boldingh, J.; Egmond, M. R. *FEBS Lett.* **1975**, *56*, 50-54.
(6) Abbreviations: TPA = tris(2-pyridylmethyl)amine; TLA = tris[(6-methyl-2-pyridyl)methyl]amine; OBz = benzoate; TBHP = *tert*-butyl hydroperoxide; CHP = cumyl hydroperoxide; TMP = tetramesitylporphyrinato dianion; dipic = 2,6-pyridinedicarboxylate; TPP = tetraphenylporphyrinato dianion.
(7) da Mota, M. M.; Rodgers, J.; Nelson, S. M. *J. Chem. Soc. A* **1969**, 2036-2044.
(8) Anal. Calcd for $C_{28}H_{29}ClFeN_4O_6$: C, 55.25; H, 4.81; N, 9.21. Found: C, 55.46; H, 4.95; N, 9.02. Anal. Calcd for $C_{52}H_{49}BFeN_4O_2$: C, 75.33; H, 5.96; N, 6.76. Found: C, 75.24; H, 6.02; N, 6.63.
(9) Crystal data for the BPh_4 salt ($C_{52}H_{49}BFeN_4O_2$·acetone, fw 886.72) at 176 K: yellow prism, monoclinic, space group $P2_1$(No.4); a = 13.347 (3) Å, b = 9.336 (5) Å, c = 18.760 (8) Å; β = 91.45 (3)°, V = 2337 (3) Å^3, Z = 2. For 9965 unique, observed reflections with $I > 2\sigma(I)$ and 557 parameters, the current discrepancy indices are R = 0.050 and R_w = 0.054.

0002-7863/93/1515-811$04.00/0

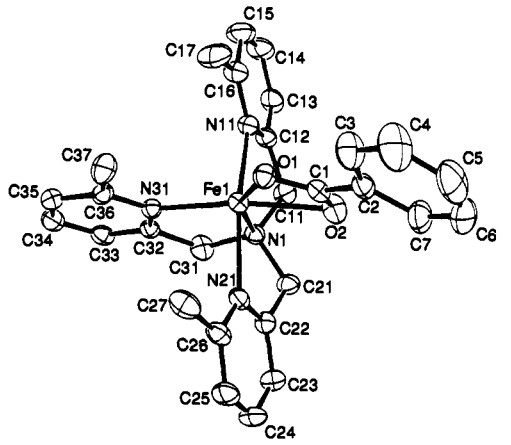

Figure 1. ORTEP drawing of the cation of **1** with atom labeling scheme. Selected bond lengths (Å) and bond angles (deg) are as follows: Fe1–O1, 2.039 (2); Fe1–O2, 2.300 (3); Fe1–N1, 2.165 (2); Fe1–N11, 2.241 (3); Fe1–N21, 2.260 (3); Fe1–N31, 2.139 (2); N31–Fe1–O1, 125.07 (8); O1–Fe1–O2, 60.23 (9); O2–Fe–N1, 92.43 (9); O2–Fe–N11, 95.25 (9); O2–Fe–N21, 83.89 (9); N1–Fe1–N11, 78.24 (9); N1–Fe1–N21, 76.52 (9); N1–Fe1–N31, 82.08 (9).

shows a six-coordinate iron with an unsymmetrically chelated benzoate (Figure 1). Steric interactions among the three methyl groups of the TLA give rise to longer average Fe–N_{py} bonds than those in the corresponding $[Fe(TPA)OAc]_2(BPh_4)_2$ complex.[10] The large N31–Fe–O1 angle (125.07 (8)°) also reflects the steric effect of the CH_3 group (C37) on the bound carboxylate. These interactions contribute to the air stability of the complex and its high redox potential (+870 mV vs NHE, irreversible in CH_2Cl_2, $Fc^{+/0}$ = +400 mV vs NHE), properties found for the ferrous center of soybean lipoxygenase.

1 reacts with TBHP or CHP at −60 °C in CH_2Cl_2 to generate the metastable pink species **2a** (λ_{max} 510 nm, ϵ_M 2300) or **2b** (λ_{max} 506 nm, ϵ_M 2300), respectively, both of which are stable at −80 °C for weeks but decompose within minutes at room temperature (Figure 2 inset). **2a** and **2b** show rhombic EPR signals at g = 4.3, which are typical of high-spin Fe(III) and account for 100% of the iron.[11] The λ_{max} of **2** appears to be insensitive to the substitution of benzoate with propionate in **1**, suggesting that the carboxylate has been displaced in **2**. UV-vis titrations of **1** with TBHP show a lag in the appearance of the chromophore until after 0.5 equiv of TBHP has been added; the chromophore is fully formed with the addition of 5 equiv. Thus, the first 0.5 equiv of ROOH oxidizes **1** to the ferric state and a subsequent equivalent replaces the carboxylate as a ligand.

The resonance Raman spectrum of **2a** in CH_2Cl_2 reveals enhanced vibrational features at 880, 844, 648, and 464 cm^{-1}, while that of **2b** shows features at 880, 832, 650, 554, and 432 cm^{-1} (Figure 2). None of the peaks is affected by the presence of $H_2{}^{18}O$. However, the use of ^{18}O-labeled CHP[12] shifts the 880, 832, and 650 cm^{-1} peaks of **2b** to 842, 804, and 626 cm^{-1}, respectively.[13] The ca. 800 cm^{-1} features are typical of peroxide O–O stretches,[14] but the isotope shifts ($\Delta\nu$ of 38 and 28 cm^{-1}, respectively) are smaller than expected for pure O–O stretches ($\Delta\nu$ of 50 and 48 cm^{-1}, respectively). Vibrational studies of the alkylperoxo moiety indicate that the O–O stretch is typically mixed with alkyl skeletal A_1 modes,[15] thereby doubling the number of features and engendering the smaller ^{18}O isotope shifts. On the basis of this vibrational data, the chromophore is assigned to a peroxo-to-Fe(III) charge-transfer band and **2** is an alkylperoxo complex.

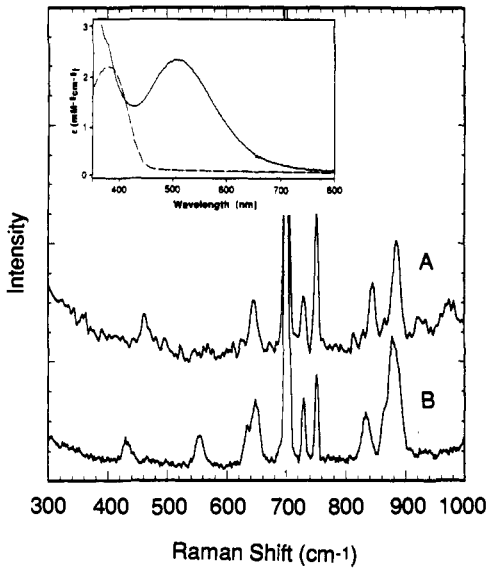

Figure 2. Resonance Raman spectra (514.5-nm excitation) of **2a** (A) and **2b** (B) in CH_2Cl_2 at 80 K. Features in the 700–760 cm^{-1} region arise from the solvent. Inset: Electronic spectra of **1** (---) and **2a** (—) in CH_2Cl_2 at −60 °C.

The 650 cm^{-1} peak is also ^{18}O-sensitive. Its position and ^{18}O isotope shift suggest its assignment to the Fe–O stretch of the FeO_2R unit. However, such vibrations are typically found near 500 cm^{-1} (e.g., ν(Fe–O_2H) = 503 cm^{-1} for oxyhemerythrin[16]), but they can be as high as 574 cm^{-1} (ν(Fe–O) for [Fe(TMP)]$_2O_2$[17]). A higher energy vibration could signify double-bond character for the Fe–O_2R bond or, more likely, an η^2 coordination mode for the alkylperoxo moiety. For the latter, the two ν(Fe–O) components of a triatomic FeO_2 moiety can couple to afford a Raman active ν_s(O–Fe–O) at higher energy than the individual ν(Fe–O)s.[18,19] The observed values for the ν_s(O–Fe–O) and its ^{18}O shift[18a] can be reproduced by employing component ν(Fe–O)s of 570 cm^{-1}, $k_{O-M-O} = 0.12k_{M-O}$, and an O–M–O angle of 45° as found for [VO(dipic)(OO-t-Bu)][20] and [Mn^{III}(TPP)(η^2-O_2)]$^-$.[21] The strength of the iron–alkyl peroxide interaction may be rationalized by the oxophilicity of an Fe^{III}TLA center having no other anionic ligands. η^2-Peroxides have also been proposed for $[Fe^{III}(EDTA)O_2]^{3-}$[22] and $[Fe^{III}(TPP)O_2]^-$;[23] unfortunately neither of these complexes exhibits a ν_s(O–Fe–O) feature.

The conversion of **1** to **2** by treatment with an alkyl hydroperoxide mimics the conversion of soybean lipoxygenase in its

(10) Ménage, S.; Zang, Y.; Hendrich, M. P.; Que, L., Jr. *J. Am. Chem. Soc.* **1992**, *114*, 7786–7792.

(11) The EPR signal was quantitated by integrating its intensity versus that of a Fe(III)(EDTA) standard at 20 K.

(12) Doubly labeled cumyl hydroperoxide was synthesized according to the procedure of Finn and Sharpless and found to be ~50% enriched as determined by mass spectroscopy. Finn, M. G.; Sharpless, K. B. *J. Am. Chem. Soc.* **1991**, *113*, 113–126.

(13) The Raman features below 600 cm^{-1}, being ^{18}O-insensitive but dependent on R, are attributed to skeletal modes of the alkyl group of the bound alkyl peroxide.

(14) Suzuki, M.; Ishiguro, T.; Kozuka, M.; Nakamoto, K. *Inorg. Chem.* **1981**, *20*, 1993–1996.

(15) Budinger, P. A.; Mooney, J. R.; Grasselli, J. G.; Fay, P. S.; Guttman, A. T. *Anal. Chem.* **1981**, *53*, 884–889.

(16) Shiemke, A. K.; Loehr, T. M.; Sanders-Loehr, J. *J. Am. Chem. Soc.* **1984**, *106*, 4951–4956.

(17) Paeng, I. R.; Shiwaku, H.; Nakamoto, K. *J. Am. Chem. Soc.* **1988**, *110*, 1995–1996.

(18) (a) Wing, R. M.; Callahan, K. P. *Inorg. Chem.* **1969**, *8*, 871–874. (b) Griffith, W. P.; Wickins, T. D. *J. Chem. Soc. A* **1968**, 397–400.

(19) The 650 cm^{-1} peak is unlikely to be the ν_{as}(O–Fe–O) because the expected strong overtone peak around 1300 cm^{-1} is not observed; neither could this feature be an alkyl skeletal mode coupled with the O–O stretch because the 650 cm^{-1} peak is insensitive to the nature of the alkyl group on the bound alkyl peroxide. Furthermore, there is no ^{18}O-sensitive peak in the 500–700 cm^{-1} region of the spectra of neat ROOH.

(20) Mimoun, H.; Chaumette, P.; Mignard, M.; Saussine, L.; Fischer, J.; Weiss, R. *Nouv. J. Chim.* **1983**, *7*, 467–475.

(21) VanAtta, R. B.; Strouse, C. E.; Hanson, L. K.; Valentine, J. S. *J. Am. Chem. Soc.* **1987**, *109*, 1425–1434.

(22) Ahmad, S.; McCallum, J. D.; Shiemke, A. K.; Appelman, E. H.; Loehr, T. M.; Sanders-Loehr, J. *Inorg. Chem.* **1988**, *27*, 2230–2233.

(23) (a) McCandlish, E.; Miksztal, A. R.; Nappa, M.; Sprenger, A. Q.; Valentine, J. S.; Stong, J. D.; Spiro, T. G. *J. Am. Chem. Soc.* **1980**, *102*, 4268–4271. (b) Frient, P.; Goulon, J.; Fischer, J.; Ricard, L.; Schappacher, M.; Weiss, R.; Momenteau, M. *Nouv. J. Chim.* **1985**, *9*, 33–40.

Fe(II) form to a purple species. The model chemistry supports the notion that the purple lipoxygenase species is a Fe(III)-linoleyl peroxide complex; however, whether the alkyl peroxide is coordinated in an η^2 fashion remains to be established by corresponding Raman studies on the enzyme complex. Metastable **2** represents the first spectroscopically characterized alkylperoxo complex of iron in a non-heme environment.[24] **2** may also be relevant to the chemistry of "activated bleomycin"[25] and that of alkane functionalization systems utilizing a combination of alkyl hydroperoxide and iron complexes.[26] The reactivity of this novel species toward a number of potential substrates is currently being investigated.

Acknowledgment. This work was supported by the National Institutes of Health (GM-33126). We thank Ms. Elizabeth C. Wilkinson for experimental assistance.

Supplementary Material Available: Tables of the atomic coordinates, thermal parameters, bond lengths, and bond angles for [Fe(TLA)(OBz)](BPh$_4$) (20 pages). Ordering information is given on any current masthead page.

(24) Nishida and Akamatsu recently reported the generation of a metastable species in the reaction of Fe(NTB)Cl$_3$ with TBHP in DMSO but did not characterize this species in detail (Nishida, Y.; Akamatsu, T. *Chem. Lett.* **1991**, 2013-2016). On the other hand, alkylperoxo complexes of iron porphyrins have been characterized; see, for example: Arasasingham, R. D.; Balch, A. L.; Cornman, C. R.; Latos-Grazynski, L. *J. Am. Chem. Soc.* **1989**, *111*, 4357-4363.

(25) (a) Hecht, S. M. *Acc. Chem. Res.* **1986**, *19*, 383-391. (b) Stubbe, J.; Kozarich, J. W. *Chem. Rev.* **1987**, *87*, 1107-1136.

(26) (a) Leising, R. A.; Norman, R. E.; Que, L., Jr. *Inorg. Chem.* **1990**, *29*, 2553-2555. (b) Leising, R. A.; Zang, Y.; Que, L., Jr. *J. Am. Chem. Soc.* **1991**, *113*, 8555-8557. (c) Vincent, J. B.; Huffman, J. C.; Christou, G.; Li, Q.; Nanny, M. A.; Hendrickson, D. N.; Fong, R. H.; Fish, R. H. *J. Am. Chem. Soc.* **1988**, *110*, 6898-6900. (d) Barton, D. H. R.; Beviere, S. D.; Chavasiri, W.; Doller, D.; Hu, B. *Tetrahedron Lett.* **1992**, *33*, 5473-5476.

A Hydrogen-Bonded, Double-Helical Macrocycle

Mark Mascal,*,† Christopher J. Moody,‡ Andrew I. Morrell,‡ Alexandra M. Z. Slawin,§ and David J. Williams§

Department of Chemistry, University of Nottingham Nottingham NG7 2RD, U.K.
Department of Chemistry Loughborough University of Technology Loughborough LE11 3TU, U.K.
Department of Chemistry Imperial College of Science, Technology and Medicine, London SW7 2AZ, U.K.

Received October 2, 1992

Helical structures are common in nature, both on the macroscopic and microscopic level. Honeysuckle (*Lonicera sempervirens*) and field bindweed (*Convolvulus arvensis*) are examples of vines which wind helically about a vertical support, the former in a left-handed and the latter in a right-handed sense. On the molecular scale, the double-helical structure of nucleic acids and the α-helix of proteins are such important and familiar architectural principles that no further discussion is warranted. Synthetic macromolecules may also adopt a helical geometry, such as is the case for both iso- and syndiotactic polypropylenes, and a host of chiral propeller molecules, helicenes, and twistanes have also been described.[1] Of particular current interest is the helical assembly around metal ions recently reported by Lehn,[2] Constable,[3] and Williams.[4] Yet to our knowledge, in no case has hydrogen bonding been analogously exploited to fix double-helical secondary structure in a nonnatural product.

Scheme I. Synthesis of Helical Azamacrocycle **1**[a]

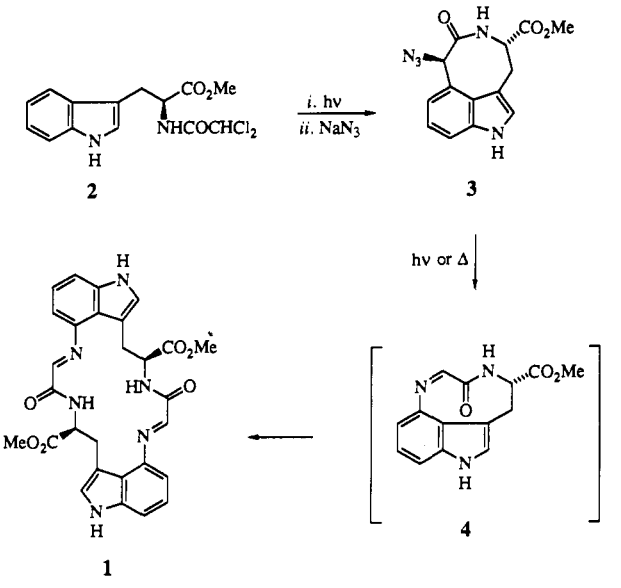

[a] A discussion of the stereochemical course of photocyclization reactions analogous to that which gives **3** is found in ref 5.

We now report the preparation of a tryptophan-derived azamacrocycle (**1**) which through strong transannular hydrogen-bonding interactions is tightly wound into the form of a left-handed double helix. A completely novel approach was taken to the synthesis of **1** as described in Scheme I. Thus, (dichloroacetyl)tryptophan methyl ester (**2**) was cyclized with UV light[5] and worked up in the presence of sodium azide to give the 7-azidopyrrolobenzazocine **3** (49%), presumably via the 7-chloro intermediate. Azide **3** could be decomposed either thermally or photochemically to provide the tetraazacyclooctadecane **1** as a result of dimerization and metathesis of strained imine **4**.[6] Well-defined, bright yellow crystals of compound **1** were grown from acetonitrile, and solution of the crystal structure[7] confirmed that the macrocycle exists in the form of a double helix (Figure 1). Models show that **1** is locked in a single conformation and cannot change screw sense without introducing serious steric interactions between the ester groups and the indole ring; thus, the tryptophan asymmetric centers direct the *M* helicity. This chirality is sacrificed on reduction of the carbon-nitrogen double bonds since the resulting diamine cannot, according to models, participate in transannular hydrogen bonding (compare $[\alpha]_D$ 1303° (*c* 0.132) in MeOH for **1** vs $[\alpha]_D$ 39° (*c* 0.125) in MeOH after reduction).

† University of Nottingham.
‡ Loughborough University of Technology.
§ Imperial College of Science, Technology and Medicine.

(1) For a comprehensive review of helical phenomena in chemistry, see: Meurer, K. P.; Vögtle, F. In *Topics in Current Chemistry*; Boschke, F. L., Ed.; Springer-Verlag: Berlin, 1985; Vol. 127, pp 1-76.

(2) Lehn, J.-M.; Rigault, A.; Siegel, J.; Harrowfield, J.; Chevrier, B.; Moras, D. *Proc. Natl. Acad. Sci. U.S.A.* **1987**, *84*, 2565. Lehn, J.-M. *Angew. Chem., Int. Ed. Engl.* **1990**, *29*, 1304 and references therein.

(3) Constable, E. C.; Ward, M. D.; Tocher, D. A. *J. Chem. Soc., Dalton Trans.* **1991**, 1675.

(4) Williams, A. F.; Piguet, C.; Bernardinelli, G. *Angew. Chem., Int. Ed. Engl.* **1991**, *30*, 1490. Rüttimann, S.; Piguet, C.; Bernardinelli, G.; Boquet, B.; Williams, A. F. *J. Am. Chem. Soc.* **1992**, *114*, 4230.

(5) Beck, A. L.; Mascal, M.; Moody, C. J.; Slawin, A. M. Z.; Williams, D. J.; Coates, W. J. *J. Chem. Soc., Perkin Trans. 1* **1992**, 797. Beck, A. L.; Mascal, M.; Moody, C. J.; Coates, W. J. *J. Chem. Soc., Perkin Trans. 1* **1992**, 813.

(6) Although compound **1** is the only product ever isolated (37%), the reaction also produces a quantity of intractable, dark yellow polymer. Correct elemental analyses were obtained for compounds **2** and **3** in addition to spectroscopic data (NMR, IR, MS, UV-vis) consistent with their structures. Compound **1** also gave a satisfactory high-resolution M$^+$.

(7) Single crystals of **1**, mp 330 ± 5 °C (rapid heating), were grown from acetonitrile and belong to the space group $C222_1$ with a = 10.696(2), b = 15.986(3), c = 17.347(3) Å, U = 2966 Å^3, D_c = 1.29 g cm^{-3}, and Z = 4 (disposed about a 2-fold axis). The structure was solved by direct methods and refined to R = 0.053, R_w = 0.054 for 1037 independent reflections.

0002-7863/93/1515-813$04.00/0